ISSN 2706-655X Vol.5, Issue 8: 8-19, DOI: 10.25236/IJFET.2023.050802

Fatigue Life Analysis of Flexible Thermal Connection Joint Bellows in Vacuum Environment for Aerospace Applications

Ying Zhou[1], Dong Liu[1], Jimin Zhang[2]

[1]China (Shanghai) Free Trade Zone Supply Chain Research Institute, Shanghai Maritime University, Shanghai, 201306, China
[2]Shanghai Institute of Satellite Engineering, Shanghai, 200240, China

Abstract: *The study focuses on the flexible thermal connection joint in the active fluid loop of spacecraft, conducting stress, stiffness, and fatigue analysis. A computational model of the flexible thermal connection joint - bellows was established and simplified through ANSYS finite element analysis, analyzing its stress, stiffness, and the stiffness coefficient correction under yield limit. Based on the Miner linear fatigue damage theory and data from the N-code fatigue analysis software library, a fatigue analysis of the bellows was carried out. The results show: the torque corresponding to the yield limit of the bellows is 132.06N, and the corresponding twist angle is 259°; the stiffness coefficient is 1.238 when not considering the effect of the torque arm, and is 1.245 when considering the effect of the torque arm; the fatigue life, fatigue safety factor, and strength safety factor of the bellows under torsional limit without preload force are all in a safe state. However, if a preload force is applied to the bellows, it may lead to an unsafe condition.*

Keywords: *Fatigue Life Analysis; Coil spring tube; Flexible Thermal Connection Joint; Vacuum Environment*

1. Introduction

The thermal environment within and outside spacecraft is complex. With the development of space technology, traditional heat conduction and radiation cooling methods such as heat pipes and coatings can no longer meet the cooling needs of high heat flux and large environments [1]. Active fluid loop cooling technology has received wide attention due to its high convective heat transfer capacity, flexible heat transfer path, and strong adaptive ability, and it has been validated in applications such as space shuttles, manned spacecraft, space stations, and deep space probes [2]. The fluid loop consists of components such as mechanical pumps, radiators, flexible thermal joints, and liquid storage devices. Mechanical pumps drive the liquid working substance to circulate in a closed loop, utilizing the sensible or latent heat of the working substance to collect, transfer, and dissipate heat [3]. Due to the special working environment of the fluid loop, the possibility of repairing components after damage is extremely low. Therefore, there are high demands for the reliability of loop components. As a moving part, the flexible thermal joint has an even higher reliability requirement.

The deployable and adjustable radiator continuously adjusts its direction according to the external heat flow direction. The liquid piping between the radiator and the fluid loop needs to have a flexible and bendable function, and this liquid piping is referred to as a flexible thermal joint. Bellows, usually made from small hollow tubing wound into springs, are typically used as flexible thermal joints. They take advantage of the elastic deformation of the tubing to achieve the pipe's flexible function and have a certain number of bending times. As the fluid transmission channel between the fluid loop and the radiator, the fatigue life of the bellows determines the overall life of the fluid loop. Studying the impact of boundary conditions and load situations on the fatigue life of the bellows has significant implications for improving the overall life of the fluid loop

Fatigue is divided into two types: high cycle fatigue and low cycle fatigue. High cycle fatigue operates at a lower stress level on parts and structural components, occurring generally between 10^4 to 10^9 loading cycles [4]. Fatigue of bellows, springs, drive shafts, etc., falls under high cycle fatigue, and for this type of fatigue, scholars often take torsion springs as the main subject of study. Dang Van proposed a method to predict fatigue life under high cycle fatigue conditions [5]. McDiamond, considering the

ISSN 2706-655X Vol.5, Issue 8: 8-19, DOI: 10.25236/IJFET.2023.050802

standards of high cycle fatigue failure, believes that cyclic load is controlled by stress [6]. Most articles mention that high cycle fatigue is a stress-controlled process, so stress must be considered an important condition when studying spring fatigue-related issues. Scholars often use time-domain and frequency-domain techniques to analyze and demonstrate the fatigue life of springs. Kong et al. used rain-flow counting in time-domain techniques to predict the fatigue life of parabolic springs in buses [7], and the time-domain rain-flow method is considered the most promising technique for predicting fatigue damage [8]. However, time-domain techniques still have some disadvantages. Time-domain-based analysis requires a vast amount of sample data to provide accurate estimates of fatigue life. Despite the reduction of analysis duration with relevant fatigue damage editing techniques, the computational cost is still high [9]. Bishop proposed a scheme to assess metal structure fatigue using frequency-domain methods [10], which require relatively fewer sample data and can speed up test times [11]. Existing teams have used this method and reverse acceleration for aluminum component durability tests, and experiments have proven that frequency-domain methods require less time and fewer data samples than time-domain methods [12]. Zhou et al. used ANSYS to establish a steel circular spring model, carried out fatigue life analysis based on Miner's linear fatigue damage theory and combined with the fatigue life software FE-SAFE, and their analysis results were consistent with reality [13]. Liu et al. predicted the fatigue life of multi-strand helical springs based on finite element analysis, verifying the reliability of the simulation scheme and the accuracy of the calculation results [14].

Numerical computation theories have gradually matured over time, and problems such as spring stiffness, stress, and fatigue are increasingly addressed using modern numerical theories, methods, and mature software technology such as finite element analysis and multibody dynamics [15]. The study of spring fatigue life has evolved from experimental data analysis to a combination of simulation analysis and experimental data. The subject of this paper is the flexible thermal joint in the active fluid loop, which has the characteristics of a spring and needs to bear the responsibility of the working substance circulation. When considering the boundary condition of applying external pressure to the spring, the internal pressure of the bellows by the working substance should also be considered. If actual experiments are used to test the fatigue life of the bellows, the test cost will be extremely high. Therefore, a fatigue life analysis should be carried out at the beginning of bellows manufacturing, and the material and structure of the bellows should be analyzed through numerical simulation analysis to extend the life of the bellows as much as possible. Although scholars at home and abroad have done a lot of work on the analysis of the fatigue life of torsion springs, research on bellows is limited, and systematic research in this area is lacking.

This paper will carry out stress, stiffness, and fatigue analysis on the bellows through ANSYS—Workbench, and combine analysis data to judge the maximum torsional angle and calculate the stiffness correction coefficient under the yield limit of the bellows to provide reference data for actual experiments. It will also calculate the fatigue life, fatigue safety factor, and strength safety factor of the bellows under conditions with and without preload force to provide suggestions for the structural design of the bellows.

2. The Computational Model, Stiffness, and Fatigue Analysis of the Bellows

The finite element analysis of the bellows is shown in Figure 1. First, it is necessary to establish a computational model, and necessary model simplifications need to be carried out to improve computational accuracy and convergence. When partitioning the finite element grid, the relationship between the quantity and density of the grid and the calculation accuracy needs to be considered. Then, corresponding boundary conditions and loads should be applied to the model according to the actual working conditions. In addition, the stiffness of the bellows is affected by the load, and its value will change and need to be corrected.

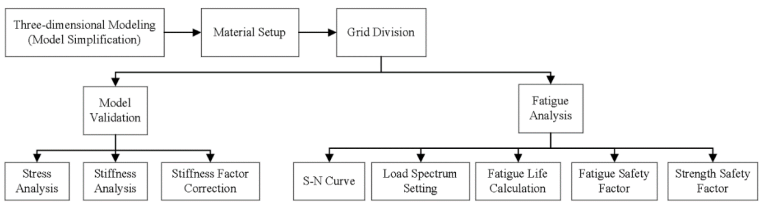

Figure 1: Analysis Flowchart

ISSN 2706-655X Vol.5, Issue 8: 8-19, DOI: 10.25236/IJFET.2023.050802

2.1 The Computational Model of the Bellows

The bellows model is three-dimensionally modeled through CATIA, as shown in Figure 2. The material is 316L stainless steel, the wire is a hollow round tube, with an outer diameter of 3mm, an inner diameter of 2.6mm, an elastic modulus of 200GPa, a shear modulus of 82GPa, and a density of 7850Kg/m³. The medium diameter of the bellows is 425mm, the number of turns is 11, and the two ends of the bellows inlet and outlet are straight pipes, each 100mm long. When the bellows is twisted, the constraints at both ends are at the end of the straight pipe section, and the range of rotation angle around the axis is from 0° to 360°, where 0° is the starting angle and 360° is the ending angle. Ideally, when the bellows is twisted, the spring only moves by contracting and expanding.

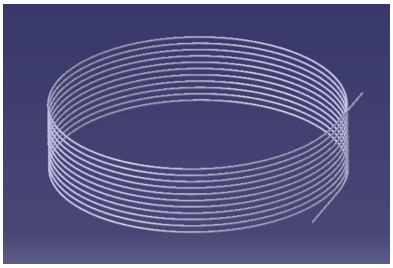

Figure 2: 3D Model of the Spiral Tube

In actual use of the bellows, the upper part needs to be fixed and the lower part rotates around the axis. To reduce the amount of computation and improve the convergence of the calculation results, the model is simplified. According to the spring design manual, the error of the arm length's effect on stiffness is within 1%, which can be ignored, so the straight pipe shape at the lower end of the bellows can be simplified by 100mm.

After simplifying the model, the bellows model needs to be partitioned with a finite element grid. The bellows is a hollow cylindrical spiral spring, with a larger diameter and a hole wall thickness of only 0.4mm. To avoid generating too many rhombuses and distorted grids, a hexahedral grid type is used. When dividing the grid, SOLID186 high-order 3D 20-node solid units are used, and a quadratic interpolation function is used to accurately control the arc curve boundary with good precision for irregular shapes. The final number of finite element units obtained is about 60,000, and the number of nodes is about 480,000, as shown in Figure 3.

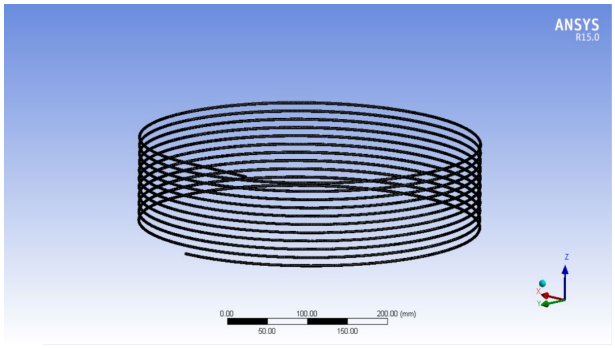

a: Overall Mesh Division of the Spiral Tube

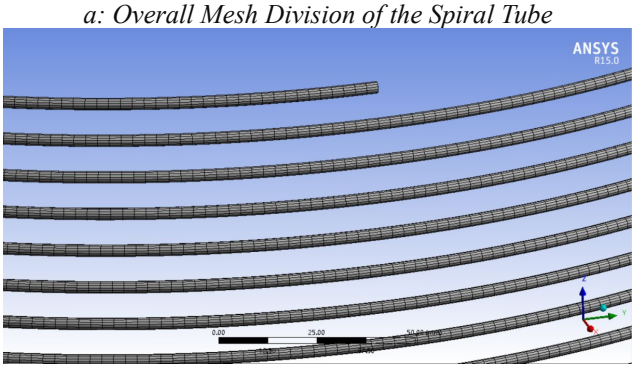

b: Local Mesh Refinement of the Spiral Tube

Figure 3: Mesh Division of the Spiral Tube

ISSN 2706-655X Vol.5, Issue 8: 8-19, DOI: 10.25236/IJFET.2023.050802

After the grid partitioning of the bellows, the corresponding boundary conditions and loads are added. The upper part of the bellows is fixed, and the lower part rotates around the axis, causing the whole to start twisting, and a gas of 1.5Mpa is applied inside the bellows. Therefore, a Fixed Support is applied to the upper part in ANSYS, the lower part is rotated around the axis, a Joint-Rotation is applied, and a pressure of 1.5Mpa is applied to the inner wall of the hollow bellows, as shown in Figure 4.

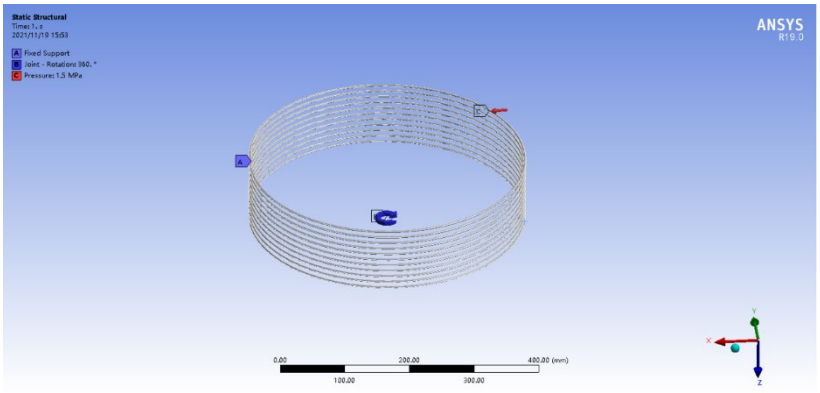

Figure 4: Applied Boundary Conditions and Load on the Spiral Tube

2.2 Stiffness Analysis of the Bellows

According to the design calculation manual for torsion springs, the theoretical stiffness of a round wire spring is2.2 Stiffness Analysis of the Bellows According to the design calculation manual for torsion springs, the theoretical stiffness of a round wire spring is

$$k = \frac{E \cdot d^4}{3667 \cdot n \cdot D} \tag{1}$$

Where, D is the central spring diameter, E is the modulus of elasticity, n is the number of working turns, and d is the wire diameter

The stiffness calculation of the bellows needs to consider its boundary conditions and load issues. Therefore, when the reinforcement effect of the gas in the pipe is not considered, the influence of the torsion arm (i.e., the straight pipe extending from the upper and lower parts) on the accuracy of the bellows is calculated.

When the influence of the torsion arm on stiffness is not considered, the theoretical calculation formula is:

$$k = \frac{E \cdot (d_1^4 - d_2^4)}{3667 \cdot n \cdot D} \tag{2}$$

When the influence of the torsion arm on stiffness is considered, the theoretical calculation formula is:

$$= \frac{\pi \cdot E \cdot (d_1^4 - d_2^4)}{3667 \cdot n \cdot D + 389 \cdot (a_1 + a_2)} \tag{3}$$

Where, d1 and d2 are the outer and inner diameters of the bellows, and a1 and a2 are the lengths of the straight pipes extending from the upper and lower parts.

When considering that the gas in the pipe has a reinforcing effect on the stiffness of the bellows, a stiffness correction coefficient ω needs to be introduced into the theoretical calculation formula for stiffness.

When the influence of the torsion arm on stiffness is not considered, the theoretical calculation formula is:

$$k = \omega \cdot \frac{E \cdot (d_1^4 - d_2^4)}{3667 \cdot n \cdot D} \tag{4}$$

When the influence of the torsion arm on stiffness is considered, the theoretical calculation formula is:

ISSN 2706-655X Vol.5, Issue 8: 8-19, DOI: 10.25236/IJFET.2023.050802

$$= \omega \cdot \frac{\pi \cdot E \cdot (d_1^4 - d_2^4)}{3667 \cdot n \cdot D + 389 \cdot (a_1 + a_2)} \tag{5}$$

There is currently no manual to check the influence of the gas on the stiffness of the bellows, and the stiffness correction coefficient cannot be obtained directly. Therefore, it is necessary to correct the theoretical calculation formula by back-calculating ω from the calculated stiffness obtained from simulation experimental data.

2.3 Fatigue Analysis

ANSYS Workbench calculates the cumulative damage based on the Miner criterion to obtain the fatigue life. The damage caused by a stress cycle with a stress amplitude of ΔS is 1/Ni, the damage caused by n stress amplitudes is ni/Ni, then the fatigue life is:

$$N_{life} = 1 \Big/ \sum_{i=1}^{n} \frac{n_i}{N_i} \tag{6}$$

The total fatigue life obtained from equation (6) is based on the input load spectrum, i.e., it will fail after the minimum number of cycles[17].

The bellows has the characteristics of springs and metal materials. The fatigue safety factor of springs and the strength safety factor calculation formula of material science can be used as references. When determining the fatigue life of the spring, the design stress of the spring and the fatigue safety factor should be considered, as shown in equation 7. When the calculation of spring design and material experimental data is highly accurate, a fatigue safety factor Smin=1.3-1.7 is used, and when the accuracy is low, Smin=1.8-2.2 is used. Due to different stress changes, the method of calculating the safety factor is also different

$$S = \frac{\tau_0 + 0.75\tau_{min}}{\tau_{max}} \tag{7}$$

Where τmin and τmax are the minimum and maximum cycle shear stresses, and τ0 is the cycle shear fatigue limit stress of the spring.

$$\tau_{min} = \frac{8kD}{\pi d^3} F_{min} \tag{8}$$

$$\tau_{max} = \frac{8kD}{\pi d^3} F_{max} \tag{9}$$

In equations (8) and (9), d denotes the diameter of the spring, and Fmin and Fmax denote the installation load and the maximum working load. When the load on the spring is continuously cycling between Fmin and Fmax, the cycle shear stress is also constantly changing.

The strength safety factor can also be referred to as the yield strength safety factor, which is generally obtained by the tensile test to get the yield strength of the material, get the stress-strain curve of the material, and get the yield strength value from the curve data. Some metal materials do not have a clear yield phenomenon as shown in Figure 5. The stress when a small amount of plastic deformation (0.2%) occurs is usually taken as the yield strength of the material, which is called the conditional yield strength[16].

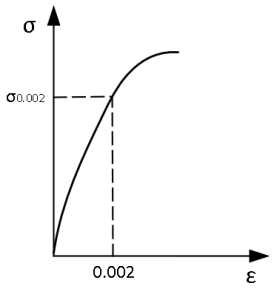

Figure 5: Stress-Strain Curve without Obvious Yield Platform

ISSN 2706-655X Vol.5, Issue 8: 8-19, DOI: 10.25236/IJFET.2023.050802

Yield strength calculation formula:

$$\sigma = \frac{F}{S} \tag{10}$$

In formula (10), F refers to the minimum force suffered by the material when it yields for plastic materials, and for brittle materials, it refers to the force suffered when the plastic deformation amount is 0.2% of the original length. S refers to the cross-sectional area of the stressed material.

3. Stress and stiffness analysis of coil springs at different angles

A computational model of the coil spring was established using ANSYS, and the stress conditions of the coil spring were obtained at 100°, 200°, 300°, and 360° rotations, respectively. As shown in Figure 6, the stress cloud map of the coil spring rotating 360°, the maximum stress occurred at the rotation place at the lower end, and the minimum stress appeared at the first coil position at the fixed end, as shown in Figures 7 and 8.

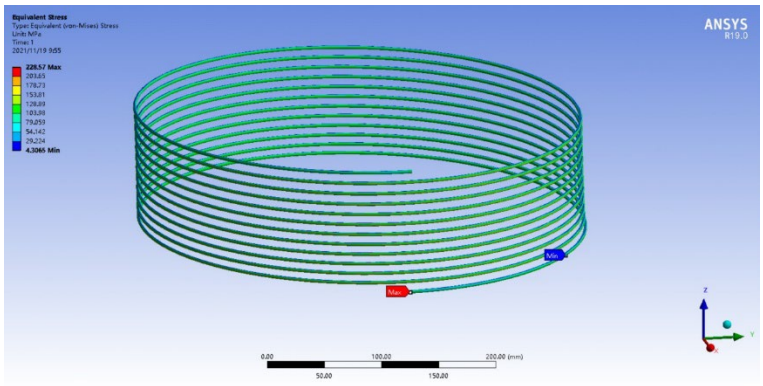

Figure 6: Stress Cloud Diagram of the Spiral Tube

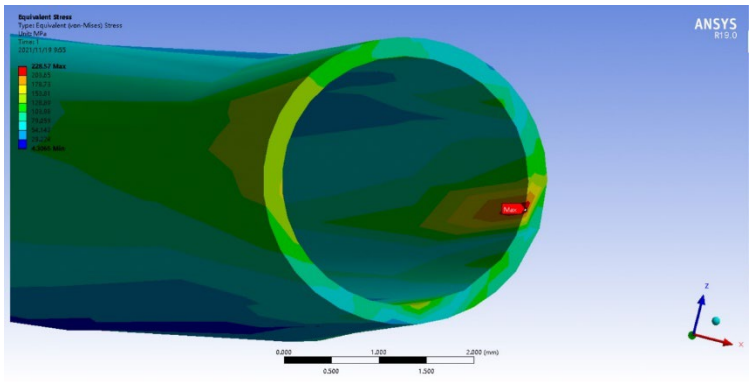

Figure 7: Location of Maximum Stress in the Spiral Tube

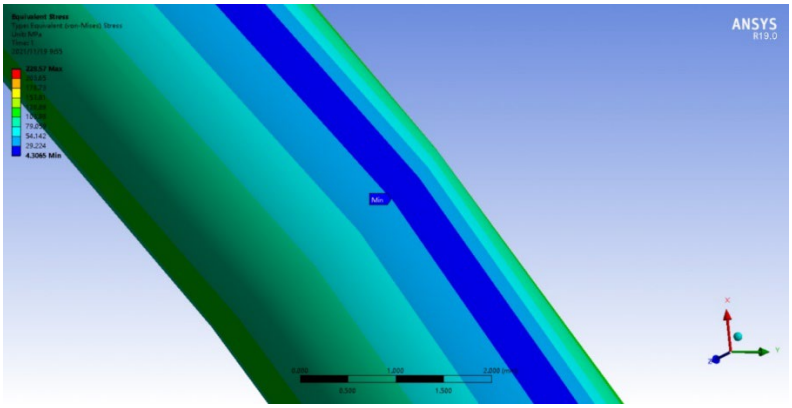

Figure 8: Location of Minimum Stress in the Spiral Tube

ISSN 2706-655X Vol.5, Issue 8: 8-19, DOI: 10.25236/IJFET.2023.050802

The stress values corresponding to different angles of rotation of the coil spring are shown in Table 1, and the line chart of the angle and stress values of the coil spring are shown in Figures 9 and 10.

Table 1: Correspondence between Angle and Stress Value

No.	Angle(°)	Stress Value(MPa)	Maximum Outer Ring Stress Value(MPa)	Maximum Inner Ring Stress Value (MPa)
1	100	86.683	45.919	86.683
2	200	140.69	86.118	140.69
3	300	197.28	126.67	197.28
4	360	228.57	150.89	228.57

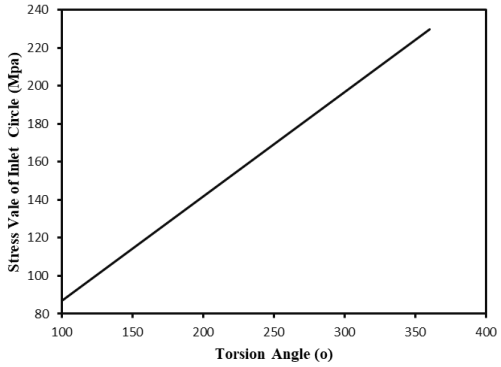

Figure 9: Angle of the Spiral Tube vs Maximum Stress Value in the Inner Ring

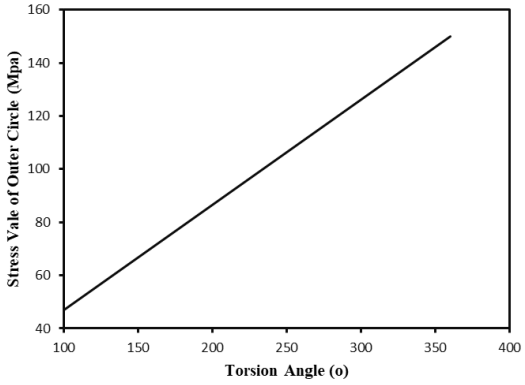

Figure 10: Angle of the Spiral Tube vs Stress Value in the Outer Ring

According to the Torsion Spring Design Manual, the yield limit of a spring made of 316L stainless steel material with a diameter of 3mm is 175MPa. As can be seen from Table 1, the maximum stress when the coil spring is twisted to 360° is 228.57MPa, which has exceeded the yield limit of the material, resulting in plastic deformation. To determine the corresponding torsional angle, maximum torque, and stiffness correction factor of the coil spring at the yield limit, the torsional angles in Table 1 were subdivided to obtain a more accurate range, as shown in Table 2.

Table 2: Relationship between Angle and Maximum Stress Value

No.	Angle/°	Stress Value/Mpa
1	255	172.19
2	256	172.76
3	257	173.33
4	258	173.9
5	259	174.47
6	260	175.04

According to the data in Table 2, when the coil spring is twisted to 259°, its maximum stress is 174.47MPa, which has reached the yield limit of the material. If it continues to twist, it will cause plastic deformation of the coil spring. Therefore, to ensure that the coil spring works within a safe range, its torsional angle is between 0° and 259°. The reliability of the stiffness analysis of the coil spring also

ISSN 2706-655X Vol.5, Issue 8: 8-19, DOI: 10.25236/IJFET.2023.050802

needs to be within the yield limit, so the torsional angle of the coil spring is analyzed to judge the stiffness of the coil spring.

Table 3: Refinement of Torsion Angle

No.	Torsion Angle(°)	Torque(N)	Stiffness(N·m)
1	20	11.939	0.596
2	40	21.483	0.537
3	60	30.887	0.515
4	80	40.243	0.503
5	100	49.662	0.496
6	120	59.252	0.494
7	140	69.102	0.494
8	160	75.259	0.47
9	180	89.72	0.498
10	200	100.42	0.52
11	220	111.24	0.505
12	240	122.01	0.508

According to the data in Table 3, the slope of the linear function curve obtained by fitting the stiffness curve is 0.51, as shown in Figure 11, so the stiffness of the coil spring is 0.51N·m.

The stiffness coefficient of the coil spring can be corrected using the data obtained from the ANSYS simulation, as shown in the following formula.

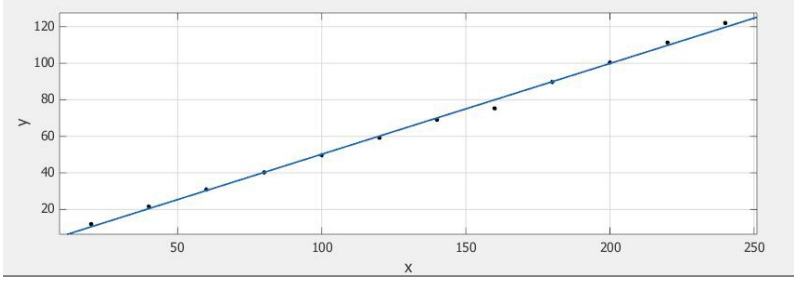

Figure 11: Stiffness Fitting Curve

When the influence of the torsion arm is not considered, $\omega = \frac{k}{\frac{E\cdot(d_1^4-d_2^4)}{3667\cdot n\cdot D}} = \frac{0.51}{0.4118} = 1.238.$

When the influence of the torsion arm is considered, $\omega = \frac{k}{\frac{\pi\cdot E\cdot(d_1^4-d_2^4)}{3667\cdot n\cdot D+389\cdot(a_1+a_2)}} = \frac{0.51}{0.4097} = 1.245.$

4. Fatigue Analysis of Coil Spring Tube

The relationship between load and fatigue failure is generally represented by the stress-life curve or S-N curve, which is typically represented logarithmically or linearly. Due to the nature of the data, logarithmic representation is generally preferred. To obtain the S-N curve of the coil spring material, as shown in Figure 12, this study analyzed the experimental results data of 316L stainless steel material in the N-code fatigue analysis software library, as shown in Table 4.

Table 4: S-N Curve Data

No.	Cycle	Alternating Stress(Pa)
1	1	1.929×10^9
2	1000	1.2026×10^9
3	10^8	4.7875×10^8
4	10^{11}	2.7549×10^8

ISSN 2706-655X Vol.5, Issue 8: 8-19, DOI: 10.25236/IJFET.2023.050802

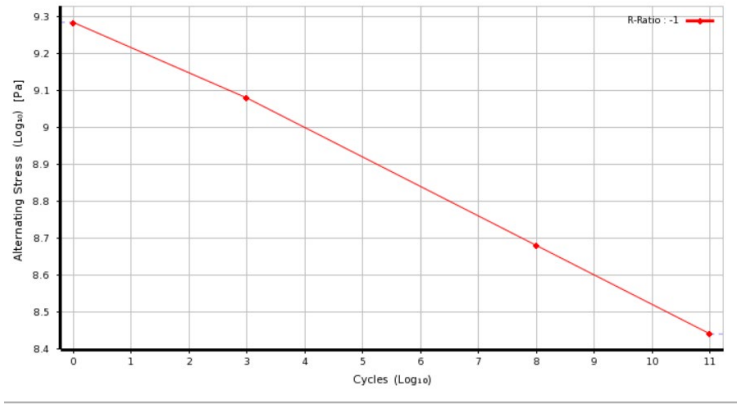

Figure 12: S-N Logarithmic Curve

The load on torsion springs is generally divided into three categories: Type I loads with more than 100,000 torsion cycles, Type II loads with 1,000-100,000 torsion cycles, and Type III loads with fewer than 1,000 torsion cycles. Considering the usage scenario and range of the coil spring, this analysis was conducted based on Type I load.

4.1 Fatigue Analysis of Coil Spring without Preload

If a rotation of 360° is taken as one cycle at a frequency of 2Hz, the calculated minimum number of fatigue life cycles for the coil spring is 47,595, as shown in Figure 13. This is less than 100,000 cycles and does not meet the standard of Type I load. If a rotation of 259° is considered as one cycle at a frequency of 2Hz, the minimum number of fatigue life cycles for the coil spring is calculated as 156.27 million, as shown in Figure 14. This number is greater than 100,000 cycles and meets the requirements of Type I load. Therefore, the fatigue safety factor and strength safety factor are calculated under the condition of satisfying Type I load, i.e., at a rotation of 259°.

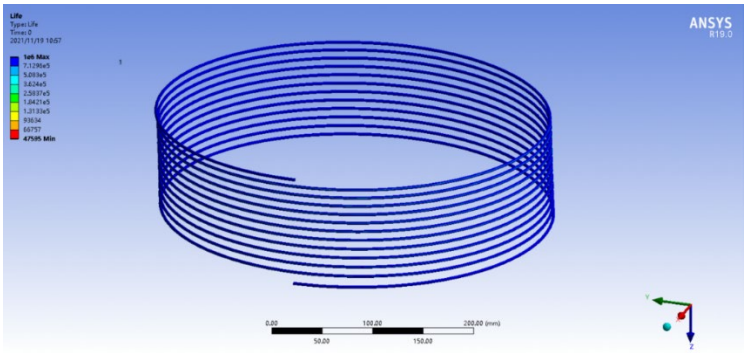

Figure 13: Fatigue Life of the Spiral Tube under 360° Twisting without Pre-tension

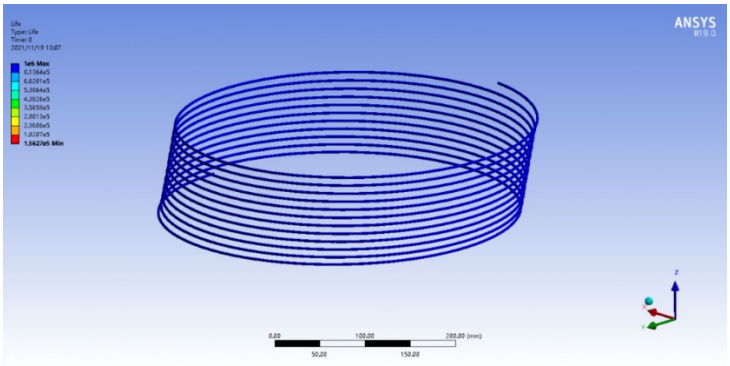

Figure 14: Fatigue Life of the Spiral Tube under 259° Twisting without Pre-tension

If the stress cycle mode is pulse cycling, taking the torsion angle from 0° to 259° as one work cycle at a frequency of 2Hz, and the number of work cycles is 100,000 times, the fatigue safety factor and strength safety factor can be obtained from this load spectrum input. The minimum fatigue safety factor

ISSN 2706-655X Vol.5, Issue 8: 8-19, DOI: 10.25236/IJFET.2023.050802

is 1.103>1, and the strength safety factor is 1.41>1, as shown in Figures 15 and 16. If the influence of the stress concentration area at the end is not considered, the fatigue safety factor and strength safety factor will be higher.

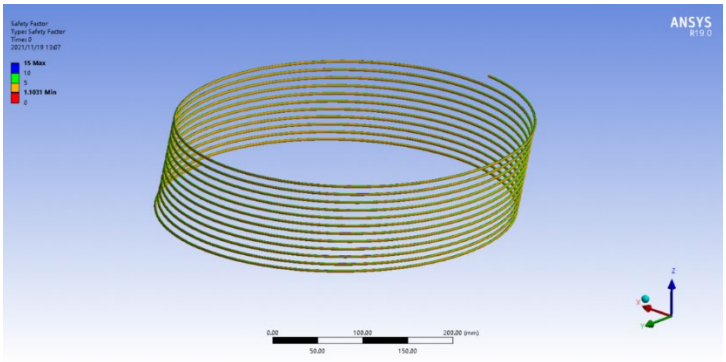

Figure 15: Fatigue Safety Factor of the Spiral Tube under 259° Twisting without Pre-tension

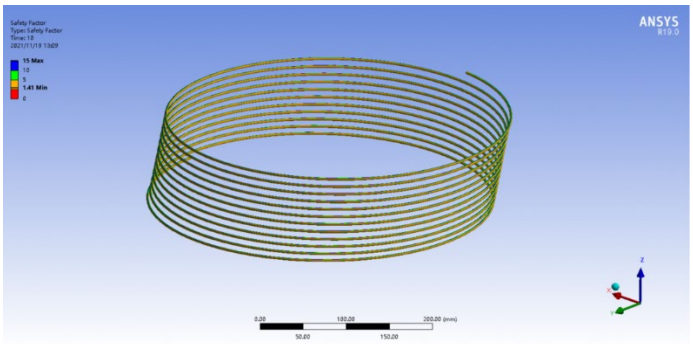

Figure 16: Strength Safety Factor of the Spiral Tube under 259° Twisting without Pre-tension

4.2 Fatigue Analysis of Coil Spring with Preload

To give the coil spring a certain preload, the initial torsion angle at the fixed end is set to 10°, so the torsion range is from 10° to 370°. The fatigue analysis data remains the same as when there is no preload. At this time, the minimum fatigue life of the coil spring after 360° rotation is 42,881, which is less than 100,000 cycles and does not meet the standard of Type I load, as shown in Figure 17.

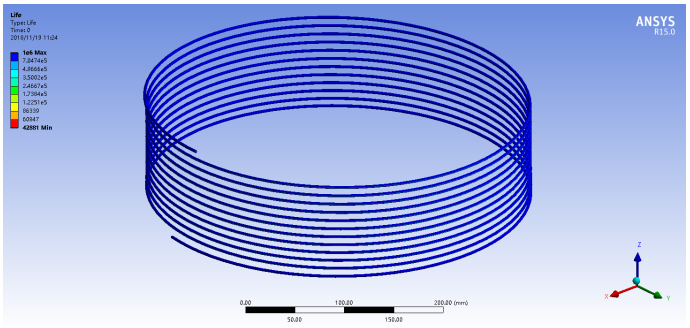

Figure 17: Fatigue Life of the Spiral Tube under 360° Twisting with Pre-tension

With the same fatigue analysis data as without preload, the fatigue safety factor of the coil spring after 360° rotation is 0.8377<1, at which point the working state of the coil spring is unsafe, as shown in Figure 18. After 360° rotation, the strength safety factor of the coil spring is 1.0707>1, at which point the coil spring is in a state of strength safety, as shown in Figure 19.

ISSN 2706-655X Vol.5, Issue 8: 8-19, DOI: 10.25236/IJFET.2023.050802

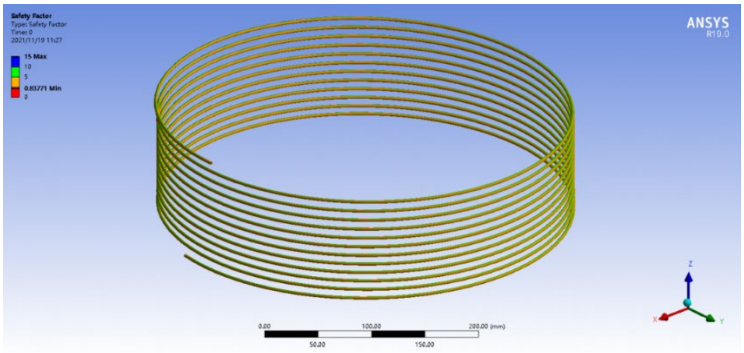

Figure 18: Fatigue Safety Factor of the Spiral Tube under 360° Twisting with Pre-tension

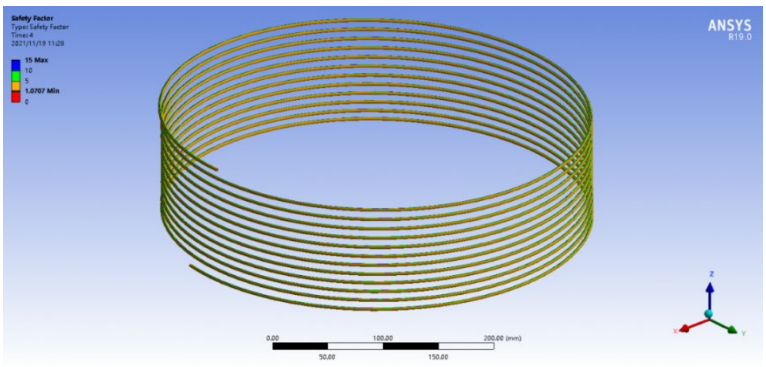

Figure 19: Strength Safety Factor of the Spiral Tube under 360° Twisting with Pre-tension

5. Conclusion

The coil spring tube has been subjected to 3D modeling, model simplification, grid partitioning, and the addition of boundary conditions. Stress and stiffness analysis of the coil spring tube at different angles were conducted, and the torsional angle and stiffness correction factor of the coil spring tube under the yield limit were obtained. Combined with the S-N curve, the fatigue life, fatigue safety factor, and strength safety factor of the coil spring tube with and without preload were analyzed. The conclusions are as follows:

(1) At a torsional angle of 360°, the maximum stress of the coil spring tube is 228.57MPa, the maximum stress on the outside is 150.89MPa, and the maximum stress on the inside is 228.57MPa. The coil spring tube experiences greater stress on the inside than on the outside during operation, so it may be considered to strengthen the material inside the tube.

(2) The torque corresponding to the yield limit of the coil spring tube is 132.06N, and the corresponding torsional angle is 259°. The working torsional angle of the coil spring tube should be controlled, or the material should be replaced to achieve the target torsional angle.

(3) The coil spring tube should avoid exceeding the limit torsional angle during operation to improve its service life. The fatigue safety factor and strength safety factor of the coil spring tube with preload are significantly reduced, and may even be in an unsafe state. Therefore, it is advisable to avoid causing the coil spring tube to twist and generate a certain preload during the assembly of the fluid circuit.

(4) The flexible thermal joint - coil spring tube simulation analysis based on ANSYS-Workbench provides some reference value for the structural design, material selection, and improvement of the life of the coil spring tube. In subsequent experiments, more boundary condition settings will be considered to provide more accurate simulation results, and they will be compared with actual experimental results.

References

[1] Jin Jian, Wang Yuning. Analysis of the influence of pipeline layout on the heat dissipation capacity of manned spacecraft radiator [J]. China Space Science and Technology, 2017, 37 (01): 66-74. DOI: 10. 16708/j. cnki. 1000-758X. 2017. 0009

ISSN 2706-655X Vol.5, Issue 8: 8-19, DOI: 10.25236/IJFET.2023.050802

[2] Xu Xianghua, Cheng Xuetao, Liang Xingang. Optimization design of the fluid circuit of the active thermal control system of manned spacecraft [J]. Journal of Astronautics and Astronautics, 2011, 32 (10): 2285-2293
[3] Ning Xianwen, Li Jindong, Wang Yuying, Jiang Fan. Review of Progress in the Construction of New Thermal Control Systems for Chinese Spacecraft [J]. Journal of Aeronautics, 2019, 40 (07): 6-18
[4] Farfan S, Rubio-Gonzalez C, Cervantes-Hernandez T, et al. High cycle fatigue, low cycle fatigue and failure modes of a carburized steel[J]. International journal of fatigue, 2004, 26(6): 673-678.
[5] Dang-Van K. Macro-micro approach in high-cycle multiaxial fatigue [J]. ASTM Special Technical Publication, 1993, 1191: 120-120.
[6] McDiarmid D L. A general criterion for high cycle multiaxial fatigue failure [J]. Fatigue & Fracture of Engineering Materials & Structures, 1991, 14(4): 429-453.
[7] Kong Y S, Omar M Z, Chua L B, et al. Fatigue life prediction of parabolic leaf spring under various road conditions[J]. Engineering Failure Analysis, 2014, 46: 92-103.
[8] Amzallag C, Gerey J P, Robert J L, et al. Standardization of the rainflow counting method for fatigue analysis[J]. International journal of fatigue, 1994, 16(4): 287-293.
[9] Liu G, Wang D, Hu Z. Application of the rain-flow counting method in fatigue[C]//2nd International Conference on Electronics, Network and Computer Engineering (ICENCE 2016). Atlantis Press, 2016: 236-240.
[10] Bishop N W M. The use of frequency domain parameters to predict structural fatigue [D]. University of Warwick, 1988.
[11] Pitoiset X, Preumont A. Spectral methods for multiaxial random fatigue analysis of metallic structures [J]. International journal of fatigue, 2000, 22(7): 541-550.
[12] Jiang Y, Yun G J, Zhao L, et al. Experimental design and validation of an accelerated random vibration fatigue testing methodology [J]. Shock and Vibration, 2015.
[13] Zhou Xinjian, Zhang Songxing. Fatigue Life Analysis of Primary Steel Circular Springs for Rapid Metro Vehicles Based on ANSYS/FE-SAFE [J]. Machine Tool and Hydraulic, 2021, 49 (01): 130-133
[14] Liu Zhipeng, Zhou Jie, Wang Shilong, Wang Sibao, Yang Wenhan. Fatigue Life Prediction of Multi Strand Spiral Springs Based on Finite Element Method [J]. China Mechanical Engineering, 2021, 32 (02): 141-146
[15] Zeng Cheng, Chen Zhongming. Analysis of the fracture problem of the primary spiral steel spring of a certain type of vehicle in Guangzhou Metro [J]. Urban Rail Transit Research, 2018, 21 (09): 145-147. DOI: 10. 16037/j. 1007-869x. 2018. 09. 037
[16] Fan Qinshan. Mechanics of Materials [M]. Beijing: Higher Education Press, 2005: 58-61
[17] Zhang Heping, Xu Wentao, Tang Yunjun, Wu Shaoning, Zhao Muqing. Fatigue Life Prediction of Micro Car Drive Axle Housing [J]. Journal of Wuhan University of Technology (Information and Management Engineering Edition), 2014, 36 (01): 57-60